

# Sustainable Energy & Fuels

Interdisciplinary research for the development of sustainable energy technologies

[rsc.li/sustainable-energy](https://rsc.li/sustainable-energy)



ISSN 2398-4902

**PAPER**

Sunita Sisodiya, Paul Hellier *et al.*  
Combustion and emissions of substituted dioxolane –  
hydrotreated vegetable oil renewable fuel blends in a  
heavy-duty diesel engine

Cite this: *Sustainable Energy Fuels*,  
2026, 10, 1419

# Combustion and emissions of substituted dioxolane – hydrotreated vegetable oil renewable fuel blends in a heavy-duty diesel engine

Sunita Sisodiya,<sup>a</sup> Nicos Ladommatos,<sup>a</sup> Amy Kittoe,<sup>b</sup> Cameron Webb<sup>b</sup>  
and Paul Hellier<sup>a</sup>

Given the accelerating pace of global warming, there is a pressing need for decarbonisation of the transport sector so as to reduce global greenhouse gas emissions. Alternative renewable fuels derived from biomass or the upcycling of waste are central to achieving this transition. Among these, molecules containing the dioxolane functional group have emerged as promising fuel candidates. Although the combustion kinetics of the dioxolane functional group have been studied, the effects of substituted dioxolanes on combustion characteristics and emissions in practical engine applications remain largely unexplored. This study presents the first experimental evaluation of 2-ethyl-2-methyl-1,3-dioxolane (2-EMD), a substituted dioxolane, as a major fuel component in a heavy-duty compression-ignition engine. 2-EMD was blended with hydrotreated vegetable oil (HVO) at 30% and 70% by volume, and tested under constant indicated mean effective pressure (IMEP) and start-of-combustion (SOC) conditions. The 30%(v/v) 2-EMD blend exhibited an ignition delay identical to that of neat HVO. However, increasing the percentage blend level of 2-EMD to 70%(v/v) resulted in a longer ignition delay and a correspondingly higher apparent peak heat release rate (PHRR), elevating NO<sub>x</sub> emissions due to increased premixed combustion. Across both blends, 2-EMD reduced incomplete combustion products (CO and THC). These findings highlight the potential of 2-EMD as a viable drop-in biofuel component for heavy-duty engines at moderate blend levels of up to at least 30%(v/v).

Received 17th November 2025  
Accepted 6th January 2026

DOI: 10.1039/d5se01530h

rsc.li/sustainable-energy

## Introduction

Heavy-duty transportation is a sector that requires urgent decarbonisation due to significant contribution of carbon dioxide (CO<sub>2</sub>) emissions from the burning of fossil fuels, particularly road freight which accounts for the majority of transport-related emissions within the European Union (EU).<sup>1</sup> Global mean surface temperatures reached unprecedented levels in 2024, marking this the hottest year on record since the beginning of modern record-keeping.<sup>2</sup> With widespread consensus among climate scientists that anthropogenic climate change is already underway, there is growing concern about the accelerating pace of global warming.

Outdoor air pollutants such as particulate matter (PM) and nitrogen oxides (NO<sub>x</sub>) contributed 7.8% of global deaths in 2019, and remained at an almost constant level since 1990 (ref. 3) despite increasingly stringent regulations controlling pollutant emissions, for example from Euro7,<sup>4</sup> and recommendations from the World Health Organisation to reduce

overall levels of atmospheric particulate matter. Therefore, a transition to cleaner renewable, low-carbon drop-in fuels is important in both, reducing pollutant emissions impacting public health and mitigating the impacts of climate change.

Substituted dioxolanes are a promising class of renewable cyclic ethers and acetals that have previously been identified as structures that can exhibit excellent fuel properties, for example, low sooting tendency and potentially enhanced engine performance through high reactivity.<sup>5–7</sup> The dioxolane functional group consists of a five-membered ring containing two oxygen atoms, forming two ether linkages as apparent in Fig. 1 showing the molecular structure of 2-ethyl-2-methyl-1,3-dioxolane (2-EMD). The combustion kinetics and properties of dioxolanes have been investigated through computational modelling and experimental data such as those from jet stirred reactor (JSR), shock tube, counterflow burner and flow reactor experiments.<sup>8–11</sup> However, to date, no studies have investigated the combustion characteristics and exhaust emissions of fuels containing the dioxolane functional group at high blend levels in a compression-ignition engine. The present study addresses this gap by evaluating, for the first time, a substituted dioxolane (2-EMD) as a major fuel component, in combination with a renewable and commercially available base fuel, hydrotreated vegetable oil (HVO).

<sup>a</sup>Department of Mechanical Engineering, University College London, Torrington Place, London, WC1E 7JE, UK<sup>b</sup>bp plc, Advanced Fluids Research, Technology Centre, Whitchurch Hill, Pangbourne, Reading, RG8 7QR, UK. E-mail: sunita.sisodiya.20@ucl.ac.uk; p.hellier@ucl.ac.uk



2-Ethyl-2-methyl-1,3-dioxolane

Fig. 1 Molecular structure of 2-ethyl-2-methyl-1,3-dioxolane (2-EMD).

Although limited, experimental studies have explored the use of 1,3-dioxolane and solketal—a hydroxyl-substituted derivative of dioxolane—as fuel blend components at low concentrations in light-duty diesel engines. Song *et al.* tested 1,3-dioxolane–diesel blends at 10% and 20% by volume, alongside glycol ether blends, alkane blends, and diesel, in a light-duty Volkswagen 1.9 L TDI engine.<sup>12</sup> The dioxolane blends produced a longer ignition delay compared to both the diesel base fuel and alkane blends (15% *n*-heptane/*n*-dodecane and 10 wt% *n*-heptane). Although there was no distinct difference in heat release between the dioxolane and alkane blends, blending 1,3-dioxolane resulted in a 5% decrease in particulate matter and slight changes in NO<sub>x</sub> and CO emissions relative to diesel. Compared to linear C<sub>4</sub>H<sub>10</sub>O<sub>2</sub> and C<sub>6</sub>H<sub>14</sub>O<sub>3</sub> glycol ether blends with similar oxygen content, the ring structure of dioxolane was less effective at reducing soot. An increase in NO<sub>x</sub> emissions was observed for both oxygenated fuel blends; however, the increase was smaller for dioxolane, likely due to lower combustion temperatures in the mixing-controlled regime and reduced oxygen release relative to glycol ether blends. This highlights the fundamental role that oxygenate molecular structure plays in emission formation, beyond oxygen content alone. Kumar *et al.* investigated solketal–biodiesel blends (up to 15% vol/vol) in a light-duty compression-ignition engine and found that solketal addition reduced incomplete combustion products, carbon monoxide (CO) and total hydrocarbons (THC), but increased nitrogen oxides (NO<sub>x</sub>) emissions and brake-specific fuel consumption (BSFC).<sup>13</sup> Türck *et al.* added solketal to diesel, biodiesel, and HVO blends and reported a reduction in cetane number (CN).<sup>14</sup> Lin *et al.* formulated nano- and micro-emulsions of solketal dispersed at 3 wt% and ultra-low sulfur diesel, reporting lower CO and NO<sub>x</sub> emissions from a direct-injection, four-stroke naturally aspirated diesel engine.<sup>15</sup> These studies demonstrate that molecular structure of dioxolanes significantly influences combustion and emissions, even at low blend levels. However, these studies were limited to light-duty engines and relatively low blend levels, and they did not examine next-generation renewable base fuels such as HVO. The present study addresses these gaps by exploring the combustion and emissions effects of 2-EMD in a heavy-duty diesel engine, and blended at varying levels with HVO, including significantly higher blend concentrations than previously reported.

## Synthesis routes for substituted dioxolanes

While a direct bio-derived route for 2-EMD has yet to be established, its precursors show promise for renewable synthesis and a variety of dioxolanes have already been successfully produced from bio-based sources.<sup>16,16,17</sup> One such method of synthesis is the catalysed acetalisation of waste glycerol with furfural obtained from lignocellulosic biomass. Glycerol is a by-product of the transesterification of vegetable oils to first-generation biodiesel, fatty acid methyl esters (FAME), comprising approximately 10% wt/wt of the total product yield, and is therefore a highly abundant yet underutilised resource, with current applications including the production of chemicals such as 1,3-propanediol used as a common solvent, in antifreeze, and cosmetics. Similarly, furfural is a major platform chemical in green chemical synthesis derived from hemicellulose, which is the second most abundant polysaccharide in lignocellulosic biomass.<sup>16</sup> Appaturi *et al.* achieved 78% specific conversion of glycerol to (2-(furan-2-yl)-1,3-dioxolan-4-yl)methanol using the reusable bifunctional catalyst MCM-41-alanine.<sup>17</sup> Similarly, Akinnowo *et al.* synthesised both 1,3-dioxolane and 1,3-dioxane *via* acetalisation of glycerol using a zirconia catalyst (ZrO<sub>2</sub> 350).<sup>18</sup>

The advancement of novel catalytic systems, including bio-based and organometallic catalysts, has opened up innovative pathways for the synthesis of dioxolanes.<sup>7,19,20</sup> Beydoun and Klankermayer produced several cyclic acetals at 93 to 98% yield by reacting various biomass-derived diols with polyoxymethylene (POM) polymers, providing an opportunity for revalorising and upcycling POM plastic waste into high-value products.<sup>19</sup> POM plastics are used in a diverse range of consumer products, with production estimated at up to 1.7 million tons annually in 2015, generating significant amounts of waste that could potentially be diverted from landfill.<sup>21</sup>

Although upcycling offers benefits in waste reduction, the carbon in fuels derived from valorised waste plastics still originates from fossil sources therefore bio-derived feedstocks are widely considered to be a more sustainable option. Fan *et al.* demonstrated that 2-alkyl-1,3-dioxolane derivatives of varying carbon chain length can also be directly produced from ethylene glycol (EG) and syngas (1 : 2 CO and H<sub>2</sub>) that can be obtained from biomass and waste glycerol in a reaction catalysed by recyclable low-cost iron nanoparticles.<sup>22</sup>

Harrison and Harvey synthesised highly reactive alkyl dioxolanes; 2,4,5-trimethyl-2-undecyl-1,3-dioxolane, 2,4-dimethyl-2-undecyl-1,3-dioxolane, and 2-methyl-2-undecyl-1,3-dioxolane, from bio-derived methyl ketones and diols *via* acid catalysed condensation.<sup>6</sup> These dioxolanes, characterised by high CN (81–91 as measured by Ignition Quality Testing, or IQT), low melting points, and comparable viscosities and net heats of combustion (NHOC) relative to conventional biodiesel, were suggested by the authors to be suitable biodiesel candidates, exhibiting good cold-temperature properties and thus the possibility of modifying the freezing point of the resulting fuel blend.

## Oxidation kinetics of dioxolanes

Cho *et al.* investigated the relationship between the chemical structure of ethers and oxidation chemistry, soot precursor



characteristics, yield sooting index (YSI) and CN.<sup>5</sup> Flow reactor experiments were performed to isolate oxidation products and elucidate kinetic mechanisms in parallel with a multivariate machine learning prediction model that generated dependencies between proposed values for YSI and CN. The latter was referred to as the fuel molecules' reactivity (indicative of auto-ignition quality) and the former a standardised metric for quantifying sooting tendency, indicative of the potential for a fuel to produce particulate matter. 2-Ethyl-4-methyl-1,3-dioxolane (EMD) and 2-isobutyl-4-methyl-1,3-dioxolane were identified as dioxolanes of low YSI, 24.0 and 45.2, respectively, compared to conventional diesel with a YSI of 246.0.

The structural properties investigated by Cho *et al.* were: cyclic *versus* acyclic structure, ring size, number and position of oxygen atoms, branching and carbon type. The carbon atom type (whether it be primary, secondary, tertiary or quaternary) and the relative position of this carbon atom to an adjacent ether oxygen atom were found to be significant features that influence YSI and CN. The model suggested that primary and secondary carbon atoms bonded to adjacent oxygen atoms were of particular importance for obtaining low YSI and high CN ethers. In the model, carbon atoms present as C–O ether linkages were predicted to be converted into carbon monoxide and were not considered to significantly contribute to soot precursor formation. In contrast, tertiary and quaternary carbon atoms were responsible for producing larger C<sub>3</sub> and C<sub>4</sub> hydrocarbon soot precursors.<sup>5</sup> Hellmuth *et al.* observed synergistic effects of 1,3-dioxolane addition on polycyclic aromatic hydrocarbons (PAH) and soot formation in ethylene counterflow diffusion flames, where soot formation increased with up to 30% dioxolane, peaking at 10%.<sup>11</sup> In agreement with Cho *et al.*, this synergistic effect of 1,3-dioxolane could be attributed to the presence of C<sub>3</sub> and C<sub>4</sub> species that form naphthalene and enable the production of larger PAH and soot.<sup>23</sup>

Alkyl chain branching was also reported to influence CN, and in acyclic (linear) ethers, branching was suggested to inhibit hydrogen migration reactions at low-temperature conditions, resulting in lower CN. In contrast, the opposite effect of branching was observed in cyclic ethers; for example, 2-isobutyl-4-methyl-1,3-dioxolane, which contains a branched structure, was found to be more reactive than 2-ethyl-4-methyl-1,3-dioxolane. The higher CN was attributed to the presence of the tertiary carbon atom in 2-isobutyl-4-methyl-1,3-dioxolane, which promoted hydrogen abstraction because of low C–H bond dissociation energy relative to the primary carbon-hydrogen bonds present.<sup>5</sup> This suggests that cyclic ethers with more branching, and thus more tertiary carbon atoms, could potentially accelerate hydrogen abstraction reactions and increase CN. However, increasing the chain length of alkyl branches has been shown to be more influential in increasing CN in dioxolanes, as measured in IQT experiments by Harvey *et al.*<sup>6,24</sup>

The presence of oxygen atoms in the dioxolane functional group, incorporated as ether linkages, was found to increase CN by enhancing OH radical production. Introducing a second oxygen atom into the molecular ring was demonstrated to significantly promote the formation of low-temperature intermediates.<sup>5</sup> It was therefore proposed that desirable fuel

candidates could be achieved by increasing the number of oxygen atoms and increasing the number of adjacent primary and secondary atoms – characteristics exhibited by 1,3,5-trioxane and also acyclic polyoxymethylene dimethyl ether. Low-temperature oxidation of the dioxolane functional group is yet to be fully understood, with most research focusing on 1,3-dioxolane (13DO), a six-membered cyclic acetal.

The heterocyclic oxygen atoms within dioxolanes have been proposed to play a dominant role in ring opening  $\beta$ -scission reactions,<sup>25</sup> consistent with the findings of Cho *et al.*<sup>5</sup> Roy *et al.* concluded that the heterocyclic oxygen atoms weaken the C–O bonds, leading to reduced barrier heights for the ring-opening reactions.<sup>25</sup> Notably, the presence of these oxygen atoms has also been reported to weaken adjacent C–H bonds, thereby promoting the formation of radicals near the oxygen atoms as well as facilitating faster internal H-atom migration from ROO to QOOH.<sup>26</sup> This was observed in 1,3-dioxane where chain propagation reaction rates exceeded chain termination, leading to higher reactivity than cyclohexane. Furthermore, Hellmuth *et al.* compared 1,3-dioxane and 1,3-dioxolane through kinetic modelling and reaction pathway analysis, supported by experimental measurements of ignition delay times, laminar flame speeds, and speciation data in a jet-stirred reactor and ethylene-based counterflow diffusion flames. In the low-temperature regime, 1,3-dioxane was found to promote degenerate chain branching, leading to the formation of keto-hydroperoxides and oxygenated species. In contrast, 1,3-dioxolane exhibited faster flame propagation and higher reactivity due to its lower C–O bond dissociation energy, which leads to direct ring-opening as the dominant pathway.<sup>10</sup> Additionally, ring strain can considerably influence the energy profiles and energy barriers of cyclic ethers during ignition reactions as compared to acyclic counterparts. For example, relative to the linear structure of diethyl ether (DEE), increased barrier heights for isomerisation reactions of peroxy radicals were reported for 1,3-dioxolane.<sup>5</sup> At high temperature, it is understood that 13DO undergoes radical chain decomposition for which rate constants have been demonstrated to be highly temperature dependent.<sup>27</sup>

Although there has been considerable interest in molecules containing the dioxolane functional group and their combustion chemistry, experimental investigations into their combustion characteristics remain limited. In particular, there is a notable absence of studies that examine exhaust emissions from practical engine applications.

To the best of the author's knowledge, there have been no previous studies on the use of a substituted dioxolane, 2-ethyl-2-methyl-1,3-dioxolane (2-EMD), as a major fuel component in a compression-ignition engine. In the study presented here, dioxolane was tested at 30% and 70% in blends with HVO at constant engine operating conditions in a heavy-duty diesel engine, with observations of the varying level of 2-EMD on combustion characteristics and gaseous exhaust emissions.

## Experimental approach

All fuels were tested in the heavy-duty engine research facility, shown in schematic form in Fig. 2, and performed at the





Fig. 2 Schematic of heavy-duty-engine test facility.

operating conditions specified in Table 3. The heavy-duty compression-ignition engine used was a six-cylinder 7.7 litre Volvo D8k (Table 1), specially modified for independent control and supply of fuel to the designated research cylinder number 1 (Fig. 2).<sup>28</sup> Control of the engine speed, injection timing and injection duration was achieved using an AVL engine timing unit (ETU) and custom electronic injector drivers. Test fuels were supplied to the research cylinder (Cylinder 1) *via* an ultra-low volume fuel system, described previously by Hellier (2013),<sup>29</sup> which utilised reference diesel pressurised by the engine common rail circuit as a hydraulic fluid acting on two free-moving pistons to test fuel injection pressure. The semi-isolated low-volume fuel delivery system allowed for operation of the engine research cylinder on test fuels available at only low quantities or having properties significantly beyond current fuel specifications such as low lubricity. The exhaust was modified and split into two separate flows. This arrangement allowed for

the isolation of emissions from the research cylinder, allowing for individual analysis of gaseous exhaust emissions using a Horiba MEXA 7000 DEGR motor exhaust analyser which measured carbon dioxide (CO<sub>2</sub>), oxygen (O<sub>2</sub>), nitrogen oxides (NO<sub>x</sub>), hydrocarbons (HC), carbon monoxide (CO) that were detected by chemiluminescence (NO<sub>x</sub>), flame ionisation detector (FID) (HC) and non-dispersive infrared (NDIR) (CO<sub>2</sub>, CO) and paramagnetic cell (O<sub>2</sub>).

In-cylinder pressure during combustion was measured by a Kistler type 6052C piezoelectric pressure transducer with its output digitised with the aid of a crankshaft encoder of resolution 0.1 crank angle degrees (CAD) (Table 1).<sup>28</sup> Integrated data acquisition and control of the experimental facility was developed in-house with a custom LabView (National Instruments) code, outlined in Deehan (2023).<sup>28</sup> Apparent net heat release rates were calculated from in-cylinder pressure data using a single zone 1st-Law thermodynamic model following the method outlined by Heywood (2018).<sup>30</sup> A custom MATLAB code, originally developed by<sup>29</sup> and later adapted by<sup>28</sup> to accommodate D8k geometries was used to plot raw in-cylinder pressure data against crank angle degrees (CAD), enabling analysis of ignition delay and combustion duration. The pressure traces were averaged over 100 consecutive combustion cycles for each test condition and subsequently used to calculate the net apparent heat release rate and in-cylinder temperature profiles during combustion, employing specific heat ratio ( $\gamma$ ) values for in-cylinder gases as reported by Heywood (2018).<sup>30</sup> Multiple datafiles were recorded during each experiment and for each

Table 1 Specification for 7.7 litre Volvo D8k research engine

Description (units)	Value
Bore (mm)	110
Stroke (mm)	135
Displacement volume (L)	7.7
Compression ratio	17.5 : 1
Number of cylinders	6
Piston bowl	Re-entrant
Shaft encoder resolution (CAD)	0.1



Table 2 Fuel properties of 2-EMD, HVO and ref. diesel

Property	2-EMD <sup>31</sup>	HVO <sup>32</sup>	Ref. diesel <sup>33</sup>
Cetane number	—	79.2	52.4
Density at 15 (°C) (kg L <sup>-1</sup> )	0.929 <sup>a</sup>	0.7803	0.8316
HHV (MJ kg <sup>-1</sup> )	31.3	48.8	47.4
LHV (MJ kg <sup>-1</sup> )	29.2	—	44.6
IBP (°C)	116	198.3	173.9
Flash point (°C)	13	76	69
Total aromatics	—	<0.2	22.6

<sup>a</sup> Density at 25 °C.

blend level, a final datafile was selected on the basis of comparable controlled conditions such as IMEP, oil temperature and fuel temperature. The fuel ignition delay was defined as the duration, in crank angle degrees (CAD), between the start of injection (SOI, defined as the time at which the injector actuating signal commences) and the start of combustion (SOC); which was defined as the time in CAD (after SOI and before the time of peak heat release rate) at which the minimum value of cumulative heat release occurs.

### Test fuels

A model substituted dioxolane was tested as a blend with HVO at two different percentage blend levels and compared to EN590-B0 reference diesel. A 70% blend level was selected to evaluate the impact of 2-EMD when it constitutes a substantial majority of the fuel blend (*i.e.*, a high blend level). A 30% blend level was also included to assess the effects at a lower blend ratio. The aim was to study the relationship between blend level and engine performance to identify the range in which significant effects occur. This work was exploratory in nature, as it represents the first study of this type conducted in an engine, and the blend selections were guided by prior experience with testing other novel fuels under similar conditions. After confirming the miscibility of HVO and 2-EMD, the fuel blends were prepared volumetrically, thoroughly mixed, and showed no evidence of phase separation at these blend levels.

In the present study, 2-ethyl-2-methyl-1,3-dioxolane (2-EMD) was selected as a representative substituted dioxolane and

available from a chemical supplier (Merck) at 99% purity and sufficient quantities required for testing in the low-volume fuel system (250 ml) (Fig. 1). The EN590-B0 reference diesel and hydrotreated vegetable oil (HVO) were sourced from bp plc.

Table 2 presents the fuel properties of 2-EMD, HVO was selected as the base fuel because it is commercially available, widely used, and representative of future fuel blends. HVO has high ignition quality, which is indicated by a cetane number of 79.2, and consists primarily of paraffinic hydrocarbons with little to no aromatic content, which in B0 diesel, contributes to soot formation during combustion<sup>34</sup> (Table 2). Among the fuels, 2-EMD had the highest density (0.929 kg L<sup>-1</sup> at 25 °C) and the lowest boiling point (116 °C) and flash point (13 °C), making it the most volatile.<sup>31</sup> In comparison, HVO had the lowest density (0.7803 kg L<sup>-1</sup>) and the highest boiling point (198.3 °C) and flash point (76 °C) (Table 2).<sup>32</sup> Further discussion regarding the fuel properties of 2-EMD is made in the context of the combustion and emissions results, for example, the impact on the premixed burn fraction.

Engine speed was set to a constant 800 rpm with a fuel injection pressure of 700 bar for all experiments. The start of combustion (SOC) was maintained at 359.7° ± 0.1°. The research engine was equipped with thermocouples to measure and record the temperatures of the oil, fuel, and air intake manifold, ensuring accurate monitoring of potential variations in the testing environment (Table 3).

To maintain a constant 8 bar IMEP, longer injection durations were required for the 2-EMD blends than those for neat HVO and diesel. Durations of 1.59 ms and 1.78 ms were required for the 30% and 70% 2-EMD/HVO blends, respectively (Table 3). Furthermore, the percentage coefficient of variation (COV) of IMEP was very low (0.57–0.58), indicating that engine operation and the combustion of these fuels was highly stable. These longer injection durations corresponded with the lower calorific values of 2-EMD compared to HVO and the B0 reference diesel (Table 2), with HHV values of 31.3, 48.8, and 47.4 MJ kg<sup>-1</sup> for 2-EMD, HVO, and B0, respectively. The lower calorific value of 2-EMD is likely due to its fuel-bound oxygen content, consistent with previous combustion studies on oxygenated fuels.<sup>35,36</sup> Gross calorific values of the fuels were determined using an IKA C1 bomb calorimeter.

Table 3 Operating conditions for 30% 2-EMD/HVO, 70% 2-EMD/HVO, HVO and ref. diesel tests at constant SOC

Parameter	30% 2-EMD/HVO	70% 2-EMD/HVO	HVO	Ref. diesel
Engine speed (rpm)	800	800	800	800
IMEP (bar)	8.09	8.04	8.07	8.09
COV in IMEP (%)	0.58	0.58	0.57	0.58
Injection pressure (bar)	700	700	700	700
Injection duration (ms)	1.59	1.78	1.52	1.51
SOI (CAD)	355.35	354.35	355.45	354.75
SOC (CAD)	359.8	359.7	359.9	359.9
Oil temp. (1) (°C)	59.2	61.8	62.7	64.5
Fuel temp. (2) (°C)	31.1	32.4	31.8	32.6
Air intake (3) (°C)	35	35	36.0	34.8



## Results and discussion

### Effects of 2-EMD blend level on combustion characteristics

Fig. 3 shows the in-cylinder pressures and heat release rates during combustion of the 2-EMD blends with HVO, neat HVO and reference diesel. Reference diesel 1 and 2 correspond to the start-of-day and end-of-day reference diesel tests, respectively. Readily apparent from Fig. 3 is that both 2-EMD blends displayed stable combustion, though that containing 70% (v/v) dioxolane exhibited a significantly higher maximum in-cylinder pressure relative to the other fuels tested and as will be seen below, this was associated with longer ignition delay and highest peak heat release rate.

At the 30%(v/v) 2-EMD blend level, the in-cylinder pressure was observed to be similar to that of neat HVO up until 366 CAD, after which the dioxolane blend exhibited a relatively higher maximum cylinder pressure comparable to reference diesel (Fig. 3a). Additionally, the apparent net heat release rate of 30% 2-EMD was largely comparable to that of neat HVO with the exception of exhibiting a larger premixed burn fraction (Fig. 3b). Similarly, Song *et al.* observed comparable heat release rates between 1,3-dioxolane–diesel blends (10% and 20% vol/vol) and alkane blends in a light-duty Volkswagen 1.9 L TDI engine.<sup>12</sup>

Notably, blending 30% 2-EMD in HVO did not change the duration of ignition delay (ID) (Fig. 4) and resulted in an ID of 4.45 (CAD), identical to that observed for neat HVO and significantly shorter than that of the reference diesel. In the case of 30%(v/v) 2-EMD in HVO, it is likely that autoignition was predominantly determined by HVO which had a high derived CN of 79.2 (Table 2). Vojtisek-Lom *et al.* observed a similar dominating influence of HVO on ignition delay in 30% butanol/HVO blends.<sup>37</sup> Therefore, at 30%, the presence of 2-EMD did not

appear to negatively influence the low-temperature reactions of HVO that lead to autoignition; the effects of 2-EMD on ignition delay are discussed further in the Discussion section. 2-EMD may also have vaporised more quickly than HVO into the gas phase due to its higher volatility (Table 2), potentially influencing the rate of air-fuel mixing and combustion dynamics. Additionally, it is suggested that the autoignition of 2-EMD in the case of the 30% blend was less dependent on the rates of low-temperature reactions, as temperatures were elevated by the ignition of HVO, which comprised the majority of fuel present. However, at a 70% 2-EMD blend level, the ignition delay (ID) was significantly longer compared to neat HVO, the 30% 2-EMD blend, and reference diesel (Fig. 4). Song *et al.* reported that the addition of 1,3-dioxolane to diesel resulted in a longer ignition delay at 10% and 20% blend levels. In contrast, the addition of 30% 2-EMD to HVO in the present study showed no change in ignition delay, suggesting that substituting ethyl and methyl groups at the 2-position of the dioxolane ring may positively influence ignition behaviour and counteract the delay associated with 1,3-dioxolane.<sup>12</sup> The impact of the 2-EMD blend on ignition delay and kinetics will be examined in greater detail in the discussion section.

Fig. 3 shows that increasing the blend ratio to 70% 2-EMD resulted in much larger premixed burn fraction and a significant increase in apparent peak heat release rate (APHRR) which also occurred earlier, as opposed to the neat HVO and 30% 2-EMD/HVO blend where the peak heat release rate occurred later during diffusion-controlled combustion. The increase in APHRR can be attributed to the longer duration of ignition delay observed for 70% 2-EMD/HVO (Fig. 4) and the greater availability of premixed fuel and air at the start of combustion, as previously observed by Hellier *et al.*<sup>38</sup>

Blending 30% 2-EMD into HVO resulted in a slightly larger heat release during the premixed burn fraction compared to neat HVO, which could be attributed to the increased volatility of 2-EMD. With a boiling point of 116 °C appreciably lower than that of HVO, the increased volatility of 2-EMD likely sped up fuel vapourisation and air-fuel mixing, resulting in a larger premixed burn fraction for an equivalent duration of ignition delay.

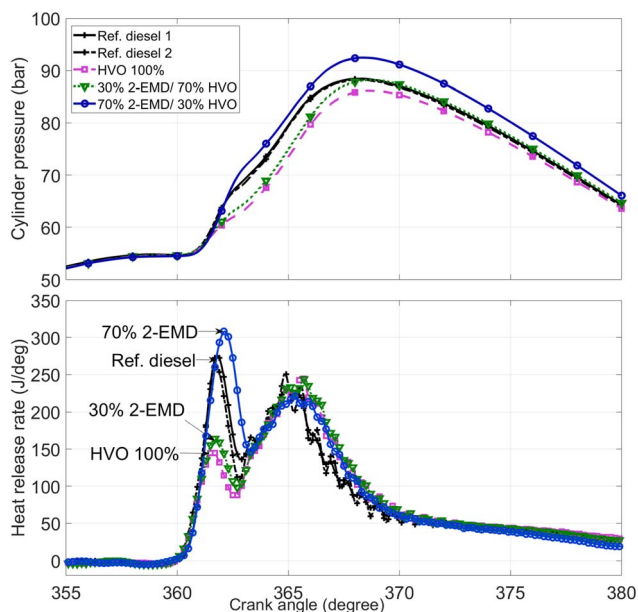


Fig. 3 (a) In-cylinder pressures and (b) apparent net heat release rates for 30% and 70% (v/v) blends of 2-EMD with HVO, neat HVO and reference diesel at constant IMEP and SOC.



Fig. 4 Duration of ignition delay for 30% and 70% (v/v) blends of 2-EMD with HVO, neat HVO and reference diesel at constant IMEP and SOC.



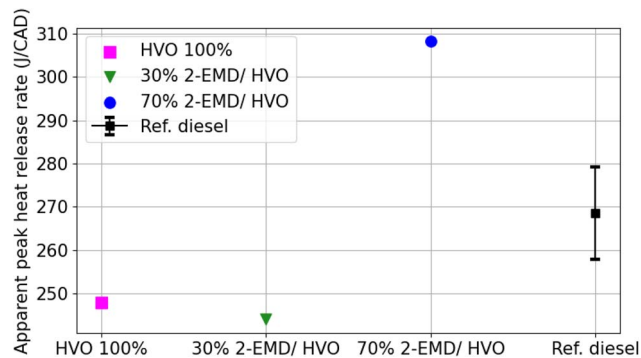


Fig. 5 Apparent peak heat release rate for 30% and 70% (v/v) blends of 2-EMD with HVO, neat HVO and reference diesel at constant IMEP and SOC.

Relative to the 70% blend, the 30% 2-EMD blend exhibited a higher peak heat release during diffusion-controlled combustion, with both the timing and magnitude of peak heat release remaining closer to that of neat HVO (Fig. 3, and 5).

### Gaseous exhaust emissions

Fig. 6 shows the nitrogen oxides (NOx) emissions, including both NO<sub>2</sub> and NO, and the level of NO only for each blend. For all tests, NO made up the majority of the NOx, with NO<sub>2</sub> levels being highest for the 70% 2-EMD blend. Fig. 7 illustrates the relationship between NOx emissions and the peak heat release rate during the premixed burn fraction for the 2-EMD blends, HVO, and reference diesel. Both neat HVO and the 30% 2-EMD/HVO blend exhibited significantly lower peak heat release rates during the premixed burn phase (Fig. 3) compared to reference diesel and emitted appreciably less NOx. However, the addition of 2-EMD increased NOx emissions, with the 70% 2-EMD blend producing higher levels than reference diesel. This is likely due to changes in combustion phasing: while neat HVO and the 30% 2-EMD blend had shorter ignition delays, the 70% 2-EMD blend ignited later, increasing the premixed burn fraction, raising peak temperatures, and promoting greater NOx formation (Fig. 7). Notably, the increased NO<sub>2</sub> emissions observed for the 70% 2-EMD blend are likely linked to higher peak temperatures, which promote NO formation *via* the thermal (Zeldovich) mechanism. The reduced PHRR observed during the mixing-controlled phase (Fig. 3) may have promoted cooler post-flame conditions conducive to NO<sub>2</sub> retention. Subsequent conversion of NO to NO<sub>2</sub> in these cooler post-flame regions facilitated by reactions with radicals such as HO<sub>2</sub> may have contributed to a greater proportion of NO<sub>2</sub> in the total NOx emissions.<sup>30,39,40</sup>

Furthermore, NOx formation appeared to be more dependent on the peak heat release rate during the premixed burn fraction than on the overall peak heat release rate during the entire combustion process, which occurred later during the diffusion-controlled phase for both HVO and the 30% 2-EMD blend (Fig. 3 and 5). Although the 30% 2-EMD blend exhibited a lower overall peak heat release rate than neat HVO, the higher heat release rate during the premixed burn fraction led to greater NOx formation (Fig. 7). This suggests that the commencement of

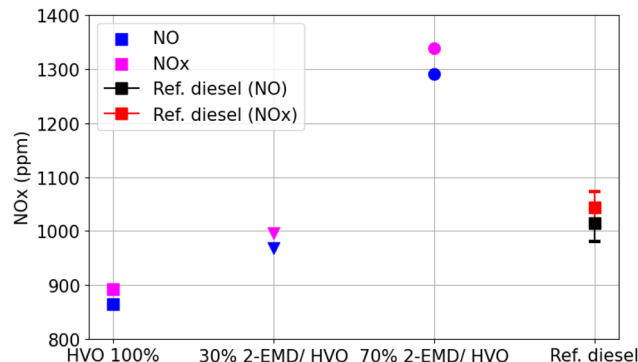


Fig. 6 Nitrogen oxides (NOx) and nitrogen oxide (NO) emissions for 30% and 70% (v/v) blends of 2-EMD with HVO, neat HVO and reference diesel at constant IMEP and SOC.

sustained elevated temperatures had a greater influence on NOx formation compared to a higher peak heat release rate achieved later during the diffusion-controlled phase. During the premixed burn phase, when in-cylinder volume is smallest, high initial heat release rates rapidly raise temperatures, which in turn accelerates NOx accumulation.

Addition of 2-EMD appeared to reduce incomplete combustion products; both the 30% and 70% 2-EMD blends emitted less CO than HVO and reference diesel, with the highest dioxolane content resulting in the largest reduction (Fig. 8). This might be attributable to the greater volatility of 2-EMD, helping to reduce fuel-rich regions, and to the presence of oxygen in the 2-EMD molecule. A similar effect of fuel oxygen content on reducing CO emissions has been previously observed in carbonate esters.<sup>41</sup> The ether linkages in 2-EMD, in which two of the carbon atoms in the ring are already bonded to oxygen as ether linkages, facilitate the oxidation of carbon atoms to carbon dioxide CO<sub>2</sub> compared to CO formation. Previous work on isotope tracing in both a pyrolyser and light-duty diesel engine has suggested that the carbon–oxygen bonds within fuel molecules often remain intact, contributing significantly less to the formation of soot. The presence of these bonds in the fuel results in the carbon being partially oxidised, requiring less additional oxygen to form CO<sub>2</sub>, thereby promoting more complete combustion.<sup>42</sup>

Furthermore, compared to 2-EMD, the higher boiling points of HVO and reference diesel (Table 2) may have resulted in greater fuel spray penetration and greater levels of fuel impingement on the cylinder walls, resulting in later and only partial combustion of the impinged fuel. Therefore, displacement of HVO with 2-EMD likely improved air-fuel mixing despite the greater relative density of 2-EMD, with relatively less mixture present within the quench zones adjacent to the walls where the temperatures might have been insufficiently high for complete combustion.

Total hydrocarbons (THC) were observed to be significantly lower for all fuels relative to reference diesel (Fig. 8). This reduction likely resulted from a more homogeneous air-fuel mixture, promoting more uniform combustion and reducing fuel-rich pockets that can cause higher THC emissions due to incomplete combustion in localised areas with insufficient oxygen. The lower





Fig. 7 Nitrogen oxides (NO<sub>x</sub>) emissions vs. peak heat release rate during the premixed burn fraction for 30% and 70% (v/v) blends of 2-EMD with HVO, neat HVO and reference diesel at constant IMEP and SOC.

boiling points of HVO and 2-EMD, compared to reference diesel (Table 2), likely contributed to improved vaporisation and combustion efficiency. Unlike conventional diesel, HVO is more homogeneous in its chemical composition which primarily consists of C16 to C18 paraffins, whereas conventional diesel contains a wider range of hydrocarbons, some of which are more difficult to vaporise and may consequently impinge on cylinder walls and crevices within the combustion chamber. Notwithstanding the range of variability in THC measurement indicated by the reference diesel, THC levels appear to decrease with 2-EMD addition to HVO and this may be due to the higher volatility of 2-EMD and improved air fuel mixing as discussed above in the context of the observed CO emissions (Fig. 8). Additionally, CO<sub>2</sub> and O<sub>2</sub> emissions were measured, with no significant variation observed across the fuel blends.

#### Discussion: impact of 2-EMD on combustion kinetics

The 30% 2-EMD blend had no apparent impact on ignition (Fig. 4), whereas the 70% 2-EMD blend exhibited a detrimental effect, underscoring the need for further investigation into the ignition kinetics of 2-EMD. Interestingly, at 30%, 2-EMD demonstrated relatively high ignition quality that matched

HVO, despite the absence of the long alkyl chains that Harvey *et al.* reported to be important for cyclic-ether ignition.<sup>6</sup> A previous study on the low-temperature chemistry of an isomer of 2-EMD, 2-ethyl-4-methyl-1,3-dioxolane, suggested that isomerisation reactions leading to the formation of keto-hydroperoxide (KHP) were thermodynamically favoured. Furthermore, the second oxygen in the ring was found to lower the energy required for the formation of low-temperature intermediates (LTIs) by up to 19.7 kcal mol<sup>-1</sup>.<sup>5</sup>

KHP decomposition is a major chain propagation pathway that occurs at a relatively lower temperature (800 K) than hydrogen peroxide (H<sub>2</sub>O<sub>2</sub>) decomposition (900–1000 K).<sup>43</sup> In the 30% 2-EMD/HVO blend, where HVO dominates and has a shorter ignition delay, most of the fuel undergoes hydrogen abstraction reactions, shifting to high-temperature conditions where 2-EMD is more reactive than at low temperatures. Below 800 K, 1,3-dioxolane is reported to exhibit low reactivity,<sup>10</sup> so HVO may help facilitate the transition to the high-temperature region, where reaction pathways such as KHP decomposition become more significant.

Therefore, the presence of 30% dioxolane in the blend may have contributed to the radical pool generated by KHP decomposition, thereby enhancing chain propagation reactions that would already be occurring in the case of the linear alkanes present in HVO, with no net effect on the observed duration of ignition delay (Fig. 4). However, the increase in ignition delay observed when increasing the 2-EMD blend to 70% and displacing the HVO suggests that autoignition was primarily driven by 2-EMD. Isomerisation reactions are known to occur most rapidly with linear alkanes, as present in HVO, due to the higher proportion of easily abstracted secondary C–H bonds.<sup>43</sup> Consequently, the reduced volume of HVO in the blend likely led to fewer hydrogen abstraction reactions, resulting in a smaller radical pool. This decrease in radicals, such as alkyl radicals and hydroperoxy radicals, reduced the availability of species required for key reactions like ring-opening and KHP formation in 2-EMD.<sup>5,10</sup> Furthermore, the decrease in HVO could have altered the composition of the radical pool, resulting in a relative increase in



Fig. 8 Carbon monoxide (CO) and total hydrocarbons (THC) emissions for 30% and 70% (v/v) blends of 2-EMD with HVO, neat HVO and reference diesel at constant IMEP and SOC.



radicals from 2-EMD. With more 2-EMD present, a larger proportion of dioxolane molecules may have undergone ring-opening through alternative decomposition pathways, potentially involving different hydroperoxy radical intermediates, as observed in the case of 1,3-dioxolane oxidation.<sup>25</sup>

At 30%, 2-EMD did not impact ignition likely because the higher HVO content provided a sufficient radical pool for normal chain propagation, following conventional steps of hydrocarbon chain branching.<sup>43</sup> However, in the 70% 2-EMD blend, the reduced HVO content resulted in a smaller radical pool, limiting the ring-opening reactions of 2-EMD and the availability of KHP. This led to a longer ignition delay, as the enhanced KHP generation from 2-EMD could not compensate for the insufficient radical pool contributed by HVO.

Although, the ignition delay was identical for both neat HVO and the 30% 2-EMD/HVO blend, the heat release rate in the premixed burn fraction was faster upon 30% 2-EMD addition, which suggests that the flame propagation for 2-EMD was faster than HVO (Fig. 3). Previous comparisons showed that the laminar flame speed of 1,3-dioxolane was faster than of ethanol, which can be advantageous for increasing engine efficiency.<sup>10</sup>

## Conclusions

This study reports tests of a substituted dioxolane (2-EMD) as a major fuel component in a compression-ignition engine, demonstrating its potential as a constituent of future low-carbon fuel blends. The following conclusions can be drawn from the results of 2-EMD combustion characterisation and gaseous exhaust emissions:

- Blending 30% 2-EMD in HVO had no significant effect on the duration of ignition delay (ID), which remained identical to neat HVO and significantly shorter than reference diesel. This suggests that, at 30% concentration, 2-EMD does not interfere with the autoignition of HVO.
- The apparent net heat release rate for the 30% 2-EMD blend was similar to neat HVO, with the exception of a larger premixed burn fraction, indicating a shift towards more premixed combustion with 2-EMD addition. The in-cylinder pressure for the 30% 2-EMD blend was similar to neat HVO until the peak energy release during diffusion-controlled combustion, after which it exhibited a higher maximum pressure, similar to reference diesel.
- The 70% 2-EMD blend exhibited the longest duration of ignition delay, which increased the apparent peak heat release rate (APHRR) in the premixed burn fraction compared to the diffusion-controlled burn observed in neat HVO and the 30% 2-EMD blend. This suggests that blending 2-EMD at high blend levels may result in a lower cetane number.
- The addition of 2-EMD to HVO appeared to reduce incomplete combustion products such as carbon monoxide (CO) and total hydrocarbons (THC), potentially due to the higher volatility of the dioxolane and a subsequent improvement in combustion efficiency at the tested blend levels.
- Neat HVO and the 30% 2-EMD/HVO blend emitted lower levels of NO<sub>x</sub> compared to reference diesel. However, the addition of 2-EMD at the higher concentration of 70% resulted in increased NO<sub>x</sub> emissions.

These findings suggest that blending 2-EMD with HVO at up to 30% does not significantly disrupt combustion dynamics and could potentially reduce certain exhaust emissions, particularly incomplete combustion products. However, higher concentrations of 2-EMD (such as 70%) may lead to increased NO<sub>x</sub> emissions due to changes in combustion timing and temperature. Further investigations into the impact of 2-EMD blends on engine performance and exhaust emissions should explore varying blend levels, especially within the range of 30% and 70%. For example, as to provide further insight into the non-linear relationship between blend level and duration of ignition delay.

## Conflicts of interest

The authors declare that there are no conflicts of interest.

## Abbreviations

2-EMD	2-Ethyl-2-methyl-1,3-dioxolane
CN	Cetane number
CO <sub>2</sub>	Carbon dioxide
CO	Carbon monoxide
HVO	Hydrotreated vegetable oil
ID	Ignition delay
IMEP	Indicated mean effective pressure
KHP	Keto-hydroxyperoxides
LTI	Low-temperature intermediates
NO <sub>x</sub>	Nitrogen oxides
POM	Polyoxymethylene
PAH	Polycyclic aromatic hydrocarbons
SOI	Start of injection
SOC	Start of combustion
THC	Total hydrocarbons
YSI	Yield sooting index

## Data availability

Data for this article, including raw in-cylinder pressure data, raw and processed temperature and emissions data, and a summary file are available at Open Science Framework and can be cited as: S. Sisodiya, P. Hellier and N. Ladommatos, 2025, Open Science Framework data repository, DOI <https://doi.org/10.17605/OSF.IO/J237U>.

## Acknowledgements

The authors thank bp plc. for financial and technological support given to this research, and also acknowledge the financial support provided by the UK Engineering and Physical Science Research Council (EPSRC).

## References

- 1 European Environment Agency (EEA), *Reducing Greenhouse Gas Emissions from Heavy-Duty Vehicles in Europe*, European Environment Agency, 2022, DOI: [10.2800/066953](https://doi.org/10.2800/066953).



- 2 G. Team, *GISS Surface Temperature Analysis (GISTEMP), version 4*, NASA Goddard Institute for Space Studies, Dataset accessed 14-Jan-2025, 2025, <https://data.giss.nasa.gov/gistemp/>.
- 3 H. Ritchie; M. Roser Air Pollution, *Our World in Data*, 2021, <https://ourworldindata.org/air-pollution>.
- 4 European Parliament and Council of the European Union Regulation (EU) 2024/1257 of the European Parliament and of the Council of 24 April 2024 on type-approval of motor vehicles and engines and of systems, components and separate technical units intended for such vehicles, with respect to their emissions and battery durability (Euro 7), amending Regulation (EU) 2018/858 and repealing Regulations (EC) No 715/2007 and (EC) No 595/2009, Commission Regulation (EU) No 582/2011, Commission Regulation (EU) 2017/1151, Commission Regulation (EU) 2017/2400 and Commission Implementing Regulation (EU) 2022/1362 (Text with EEA relevance), *Off. J. Eur. Communities: Legis.*, 1257, 8 May 2024, 2024, PE/109/2023/REV/2, <http://data.europa.eu/eli/reg/2024/1257/oj>.
- 5 J. Cho, Y. Kim, B. D. Etz, G. M. Fioroni, N. Naser, J. Zhu, Z. Xiang, C. Hays, J. V. Alegre-Requena and P. C. S. John, others Bioderived ether design for low soot emission and high reactivity transport fuels, *Sustainable Energy Fuels*, 2022, **6**, 3975–3988.
- 6 K. W. Harrison and B. G. Harvey, High cetane renewable diesel fuels prepared from bio-based methyl ketones and diols, *Sustainable Energy Fuels*, 2018, **2**, 317–500.
- 7 M. Nicolas, N. Gaelings, J. Wiesenthal, W. G. von Westarp, B. Pehlivanlar, S. Pischinger, A. Jupke, J. Klankermayer and D. Rother, Combination of Bio-and Organometallic Catalysis for the Synthesis of Dioxolanes in Organic Solvents, *ChemCatChem*, 2025, e202401836.
- 8 H. Kwon and Y. Xuan, Pyrolysis of bio-derived dioxolane fuels: A ReaxFF molecular dynamics study, *Fuel*, 2021, **306**, 121616.
- 9 A. Wildenberg, M. Döntgen, I. S. Roy, C. Huang, B. Lefort, L. L. Moyne, A. Kéromnès, K. Leonhard and K. A. Heufer, Solving the riddle of the high-temperature chemistry of 1,3-dioxolane, *Proc. Combust. Inst.*, 2023, **39**, 705–713.
- 10 M. Hellmuth, B. Chen, C. Bariki, L. Cai, F. Cameron, A. Wildenberg, C. Huang, S. Faller, Y. Ren and J. Beeckmann, others A comparative study on the combustion chemistry of two bio-hybrid fuels: 1, 3-dioxane and 1, 3-dioxolane, *J. Phys. Chem. A*, 2022, **127**, 286–299.
- 11 M. Hellmuth, F. Cameron, S. Faller, L. Schmückert, B. Chen, Y. Ren and H. Pitsch, Synergistic effect on PAH and soot formation in ethylene counterflow diffusion flames by the addition of 1, 3-dioxolane-a bio-hybrid fuel, *Proc. Combust. Inst.*, 2023, **39**, 899–908.
- 12 J. Song, V. Zello, A. L. Boehman and F. J. Waller, Comparison of the impact of intake oxygen enrichment and fuel oxygenation on diesel combustion and emissions, *Energy Fuels*, 2004, **18**, 1282–1290.
- 13 P. Kumar, S. Kumar, S. Shah and S. Kumar, Study of performance parameters and emissions of four stroke CI engine using solketal-biodiesel blends, *SN Appl. Sci.*, 2021, **3**, 1–8.
- 14 J. Türck, A. Singer, A. Lichtinger, M. Almaddad, R. Türck, M. Jakob, T. Garbe, W. Ruck and J. Krahl, Solketal as a renewable fuel component in ternary blends with biodiesel and diesel fuel or HVO and the impact on physical and chemical properties, *Fuel*, 2022, **310**, 122463.
- 15 C.-Y. Lin and S.-M. Tsai, Emission characteristics of a diesel engine fueled with nanoemulsions of continuous diesel dispersed with solketal droplets, *J. Environ. Sci. Health, Part A*, 2020, **55**, 224–229.
- 16 A. E. Eseyin, and P. H. Steele, *An Overview of the Applications of Furfural and its Derivatives*, 2015.
- 17 J. N. Appaturi, R. J. Ramalingam, H. A. Al-Lohedan, F. Khoerunnisa, T. C. Ling and E. P. Ng, Selective synthesis of dioxolane biofuel additive via acetalization of glycerol and furfural enhanced by MCM-41-alanine bifunctional catalyst, *Fuel*, 2021, **288**, 119573.
- 18 C. A. Akinnawo, L. Mosia, O. A. Alimi, C. O. Oseghale, D. P. Fapojuwo, N. Bingwa and R. Meijboom, Eco-friendly synthesis of valuable fuel bio-additives from glycerol, *Catal. Commun.*, 2021, **152**, 106287.
- 19 K. Beydoun and J. Klankermayer, Efficient Plastic Waste Recycling to Value-Added Products by Integrated Biomass Processing, *ChemSusChem*, 2020, **13**, 488–492.
- 20 K. Beydoun and J. Klankermayer, Ruthenium-Catalyzed Synthesis of Cyclic and Linear Acetals by the Combined Utilization of CO<sub>2</sub>, H<sub>2</sub>, and Biomass Derived Diols, *Chem.–Eur. J.*, 2019, **25**, 11412–11415.
- 21 D. L. P. Jarvis, *Brydson's Plastics Materials*, 8th edn, 2017, pp. 513–526.
- 22 X.-B. Fan, N. Yan, Z.-Y. Tao, D. Evans, C.-X. Xiao and Y. Kou, One-Step Synthesis of 2-Alkyl-dioxolanes from Ethylene Glycol and Syngas, *ChemSusChem*, 2009, **2**, 941–943.
- 23 M. Hellmuth, R. Langer, A. Meraviglia, J. Beeckmann and H. Pitsch, The role of C<sub>3</sub> and C<sub>4</sub> species in forming naphthalene in counterflow diffusion flames, *Proc. Combust. Inst.*, 2024, **40**, 105620.
- 24 O. Staples, C. M. Moore, J. H. Leal, T. A. Semelsberger, C. S. McEnally, L. D. Pfefferle and A. D. Sutton, A simple, solvent free method for transforming bio-derived aldehydes into cyclic acetals for renewable diesel fuels, *Sustainable Energy Fuels*, 2018, **2**, 2742–2746.
- 25 I. S. Roy, M. Döntgen, C. Huang, W. Kopp and K. Leonhard, Influence of Oxygen Atoms and Ring Strain on the Low-Temperature Oxidation Pathways of 1,3-Dioxolane, *J. Phys. Chem. A*, 2023, **127**(13), 2992–2999.
- 26 C. Huang, Y. Zhao, I. S. Roy, L. Cai, H. Pitsch and K. Leonhard, Effect of methyl substituents, ring size, and oxygen on bond dissociation energies and ring-opening kinetics of five- and six-membered cyclic acetals, *Combust. Flame*, 2022, **242**, 112211.
- 27 M. Adil, B. R. Giri, T. V. Mai, M. Szőri, L. K. Huynh and A. Farooq, High-temperature mid-IR absorption spectra and reaction kinetics of 1,3-dioxolane, *Proc. Combust. Inst.*, 2023, **39**, 621–631.



- 28 T. Deehan, *Investigating the Combustion and Emission Characteristics of Lignocellulosic Derived Future Fuels with Novel Chemical Reactivity in a Heavy-Duty Compression Ignition Engine*, PhD thesis, University College London, 2023.
- 29 P. Hellier, *The Molecular Structure of Future Fuels*, PhD thesis, University College London, 2013.
- 30 J. B. Heywood, *Internal Combustion Engine Fundamentals*, McGraw-Hill Education, 2018.
- 31 2-Ethyl-2-methyl-1,3-dioxolane Safety Data Sheet 341045, 2024, <https://www.sigmaaldrich.com/GB/en/product/aldrich/341045?srsId=AfmBOorvQGoZUafzX7nApfK31ZuYte-BpK9ODD6bjlJ8lVctGtbh4eKv>.
- 32 *Certificate of Analysis*, BP HVO, 2022.
- 33 *Certificate of Analysis*, BP EN590 B0, 2022.
- 34 D. R. Tree and K. I. Svensson, Soot processes in compression ignition engines, *Prog. Energy Combust. Sci.*, 2007, **33**, 272–309.
- 35 A. K. Agarwal, A. Dhar, J. G. Gupta, W. I. Kim, K. Choi, C. S. Lee and S. Park, Effect of fuel injection pressure and injection timing of Karanja biodiesel blends on fuel spray, engine performance, emissions and combustion characteristics, *Energy Convers. Manage.*, 2015, **91**, 302–314.
- 36 T. Deehan, P. Hellier and N. Ladommatos, The influence of Michael acceptors on the structural reactivity of renewable fuels, *Sustainable Energy Fuels*, 2024, **8**, 4168–4182.
- 37 M. Vojtisek-Lom, V. Beránek, P. Mikuška, K. Křůmal, P. Coufalík, J. Sikorová and J. Topinka, Blends of butanol and hydrotreated vegetable oils as drop-in replacement for diesel engines: Effects on combustion and emissions, *Fuel*, 2017, **197**, 407–421.
- 38 P. Hellier, N. Ladommatos, R. Allan, M. Payne and J. Rogerson, The impact of saturated and unsaturated fuel molecules on diesel combustion and exhaust emissions, *SAE Int. J. Fuels Lubr.*, 2012, **5**, 106–122.
- 39 Y. Zeldovich, D. Frank-Kamenetskii, and P. Sadovnikov, *Oxidation of Nitrogen in Combustion*, Publishing House of the Acad of Sciences of USSR, 1947.
- 40 C. T. Bowman, Kinetics of pollutant formation and destruction in combustion, *Prog. Energy Combust. Sci.*, 1975, **1**, 33–45.
- 41 P. Hellier, N. Ladommatos, R. Allan and J. Rogerson, Influence of carbonate ester molecular structure on compression ignition combustion and emissions, *Energy Fuels*, 2013, **27**, 5222–5245.
- 42 A. Eveleigh, N. Ladommatos, P. Hellier and A.-L. Jourdan, Quantification of the fraction of particulate matter derived from a range of <sup>13</sup>C-labeled fuels blended into heptane, studied in a diesel engine and tube reactor, *Energy Fuels*, 2016, **30**, 7678–7690.
- 43 C. K. Westbrook, Chemical kinetics of hydrocarbon ignition in practical combustion systems, *Proc. Combust. Inst.*, 2000, **28**, 1563–1577.

